

Chapter 2

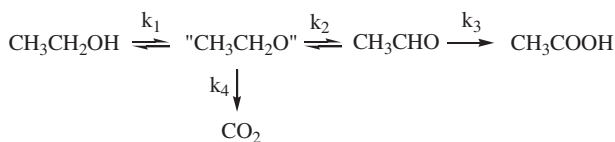
Selective Oxidation/Dehydrogenation Reactions

2.1 Primary Alcohol and Aldehyde Oxidation

2.1.1 Ethanol Oxidation

Selective oxidation of ethanol results in the formation of acetaldehyde, 1,1-diethoxyethane, acetic acid, and ethyl acetate. Currently, 75 % of acetic acid is formed via methanol carbonylation utilizing fossil resources and 25 % by classical fermentation [1]. Ethyl acetate has a wide range of applications in different areas including the paint and food industries [2]. Gold catalysts were found to be active and selective in the synthesis of both acetic acid and ethyl ester in the presence of oxygen [3, 4]. Moreover, the use of gold catalysts allowed for the use of less severe reaction conditions compared to those needed for other catalysts active in the gas-phase such as supported V_2O_5 (175–200 °C, 270 kPa), Nb-Mo-V-Ox (237 °C, 1600 kPa) [5–7]. It is important to note that the product composition depends on the reaction conditions employed as well as the nature of the catalysts, including the metal particle size and the composition of the support.

Aerobic oxidation of aqueous ethanol to acetic acid over Au/MgAl₂O₄ and Au/TiO₂ was studied by Christensen and coworkers [3, 4]. For both catalysts, the yield of acetic acid was over 90 % at high ethanol conversion. The reaction was performed at 150 °C, under technical air pressure of 3.5 MPa. The kinetics of acetic acid formation were investigated and were consistent with the following proposal regarding the reaction mechanism. As a first step, ethanol is adsorbed on the gold surface to form activated intermediate species, which then is oxidized/dehydrogenated to the aldehyde. Consequently, aldehyde is oxidized to acetic acid, while CH₃CH₂O can also undergo C–C bond cleavage to produce CO₂ (Scheme 2.1). The selectivity was influenced by the ethanol concentration. At ethanol concentration lower than 60 wt. %, the major product was acetic acid, whereas when the concentration exceeded 60 wt. %, the selectivity shifted towards ethyl acetate [4].

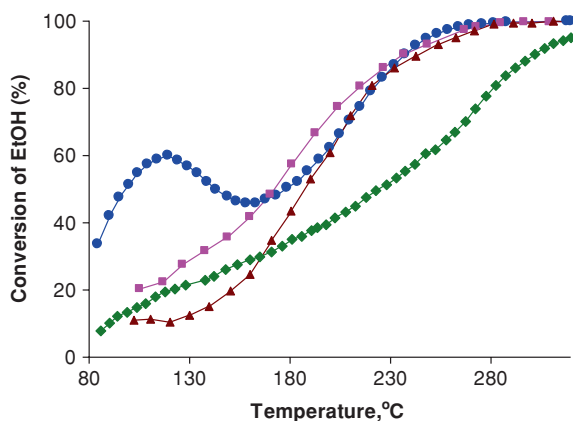


Scheme 2.1 The reaction pathway of ethanol oxidation over Au catalysts. Reprinted from Ref. [3], Copyright © 2007, with permission from Elsevier

Oxidation of alcohols over gold catalysts at temperatures lower than 150 °C is typically performed in the liquid-phase [8–11]. However, a solvent-free reaction is more attractive from industrial point of view. The reaction temperatures currently used for selective oxidation of gas-phase ethanol are generally above 200 °C over various Au catalysts, which leads to catalyst deactivation. Therefore, the low-temperature activity of Au/TiO₂ catalysts in gas-phase ethanol oxidation observed in [12] seems to be promising for practical application. A so-called ‘double peak’ catalytic activity was observed only in case of titania-supported gold catalyst and represents the unusual activity in gas-phase at 120 °C and the expected one at temperature above 200 °C (Fig. 2.1).

To understand the catalytic function of gold, the mechanism of gas-phase oxygen activation was studied by oxygen isotope exchange (OIE) technique by Sobolev et al. [13]. The low-temperature activity of the catalyst in homo-exchange can indicate the involvement of very active surface oxygen species. It should be noted that Au/TiO₂ and Au/Al₂O₃ have demonstrated similar activity in ethanol dehydrogenation at low temperature (75 °C), while Au/SiO₂ was not active at the same conditions. Interactions of Au/TiO₂ surface oxygen atoms with hydrogen from the gas-phase resulted in the formation of water at 150 °C. Furthermore, Au/TiO₂ pretreated in hydrogen is able to catalyze oxygen isotope homo-exchange at room temperature, while the equilibrium of the exchange can be reached in a few minutes. Similar to Au/TiO₂ catalyst Au/Al₂O₃ has demonstrated activity

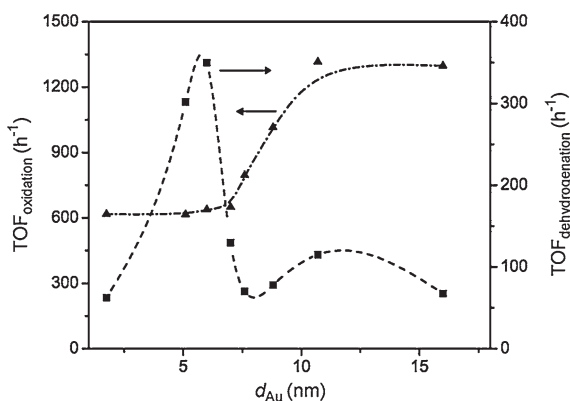
Fig. 2.1 Ethanol conversion over TiO₂ (filled triangle), 2 wt. % Au/TiO₂ (filled circle), 2 wt. % Au/Al₂O₃ (filled square), 1 wt. % Au/SiO₂ (filled diamond). Reprinted from Ref. [12], Copyright © 2010 Wiley-VCH Verlag GmbH & Co. KGaA, Weinheim



in oxygen isotope homo-exchange, although not significant. In the studied reaction Au/SiO₂ was not active at all. Catalyst pretreatment by molecular hydrogen led to formation of active oxygen species on the surface of titania and alumina. Although the exact nature of these species is unclear, they might be O^{•−} anion radicals or O₂^{•−} superoxide ions. The thermal stability of these species on Al₂O₃ is much lower than those on TiO₂. It was assumed that formation of surface oxygen species and their stability are the key factors responsible for the differences in catalyst performance among the various supported samples and higher catalytic activity of Au/TiO₂ at low temperature. Moreover, the activity of titania-supported gold in ethanol dehydrogenation allows additional in situ hydrogen formation thus enhancing oxidizing surface species formation. The thermostability of active oxygen species was estimated based on the temperature dependence of the oxygen isotope homo-exchange rate, which is proportional to the amount of active surface oxygen. In contrast to Al₂O₃, TiO₂ surface provides the essential thermostability of the generated oxygen species.

Structure sensitivity and kinetics of ethanol oxidative dehydrogenation in aerobic and anaerobic conditions were thoroughly studied by Guan et al. [14]. Silica-supported gold catalysts (with and without aluminum impurities) were applied in the temperature range 150–400 °C. The gold particle size was varied between 1.7 and 15 nm. Ethanol dehydrogenation had a selectivity of 100 % at temperatures below 350 °C, and was still over 90 % at 400 °C. The highest activity per exposed site was obtained over a gold catalyst with a metal particle size of about 6 nm. The calculated turnover frequency (TOF) for ethanol dehydrogenation at 250 °C was 350 h^{−1} while the achieved selectivity to acetaldehyde was 95 % at a conversion of 90 %. The presence of molecular oxygen significantly promoted the reaction rate and lowered the apparent activation energy. The TOF of oxidative dehydrogenation was four times higher (1300 h^{−1} at 200 °C). Catalytic activity dependence on the particle size was also different and increased with increasing particle size up to 10 nm (Fig. 2.2). Selectivity to acetaldehyde was 90 % at about 100 % of ethanol conversion.

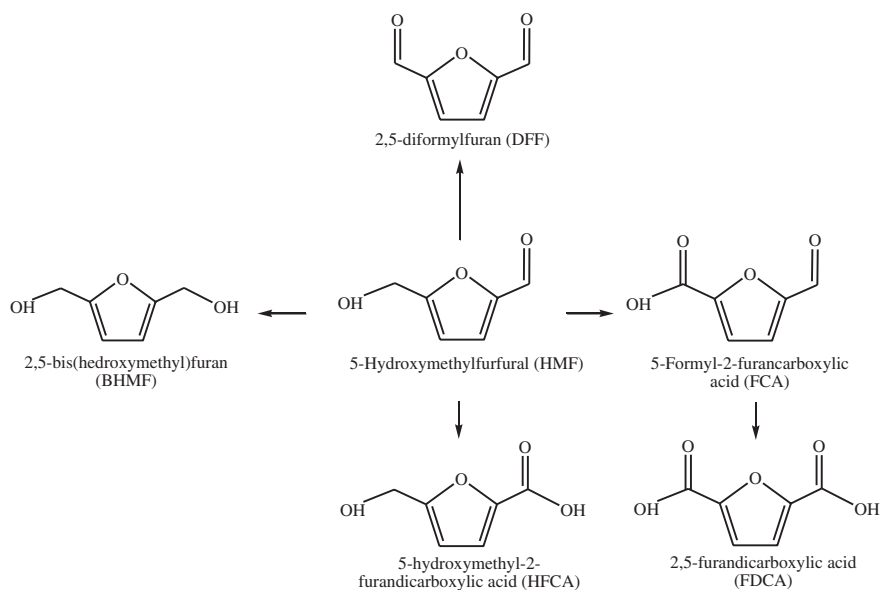
Fig. 2.2 Turnover frequency (TOF) for ethanol dehydrogenation in the absence (*filled square*, 250 °C) and presence (*filled triangle*, 200 °C) of oxygen as a function of the gold particle size. Reprinted from Ref. [14], Copyright © 2009, with permission from Elsevier



2.1.2 5-Hydroxymethyl-2-Furfural Oxidation

The selective oxidation of HMF was studied over various catalysts such as Pt–Pb, Pt/Al₂O₃, Pd, metal bromide catalysts (Co/Mn/Zn/Br), vanadyl-pyridine complexes [15–18]. In general, FDCA production proceeds in two stages: first, the aldehyde group is oxidized to 5-hydroxymethyl-2-furancarboxylic acid (HFCA), and consequently FDCA is formed from the primary alcohol group oxidation (Scheme 2.2). Typically, the first stage is much faster than the second one. Another detected intermediate is 5-formyl-2-furancarboxylic acid (FCA). Catalysts based on transition metals can be deactivated due to over oxidation of the metal surface. In case of nontransition metals as catalysts the main product was reported to be 2,5-diformylfuran (DFF) with selectivity of 99 % at mild temperature (50–75 °C) and FDCA with selectivity higher than 97 % and yield of ca. 60 % at higher temperatures (100–225 °C). Notably, basic pH is favorable for FDCA production.

Since oxidation of HMF to FDCA is in fact selective oxidation of two groups: primary alcohol and aldehyde, where gold catalysts have demonstrated high activity and selectivity, several attempts to apply Au catalyst were reported. Oxidation of HMF over Au/TiO₂ in methanol at 130 °C in the presence of base was reported by Taarning et al. [19]. Gorbanev et al. [20] also reported utilization of Au/TiO₂ at 30 °C, while the reaction was performed in aqueous solutions with NaOH to HMF molar ratio of 20. Increasing oxygen pressure from 1000 to 2000 kPa boosted the FDCA yield up to 71 % at full HMF conversion. Selective oxidation of HMF in



Scheme 2.2 Products of HMF oxidation. Reprinted from Ref. [22]. Copyright © 2011, with permission from Elsevier

aqueous solutions was investigated over Au/TiO₂, Au/CeO₂, Au/C, Au/FeO₂ by Casanova et al. [21]. In this series of catalysts the best results were obtained over Au/TiO₂ and Au/CeO₂ catalysts. The yield of FDCA was more than 99 % after 8 h over Au/CeO₂. The optimized reaction conditions were found to be 130 °C, 1000 kPa oxygen, and the NaOH to HMF molar ratio equals to 4.

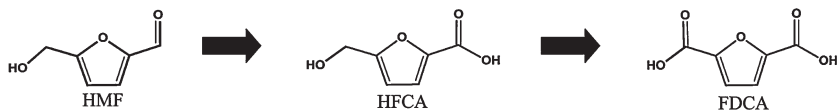
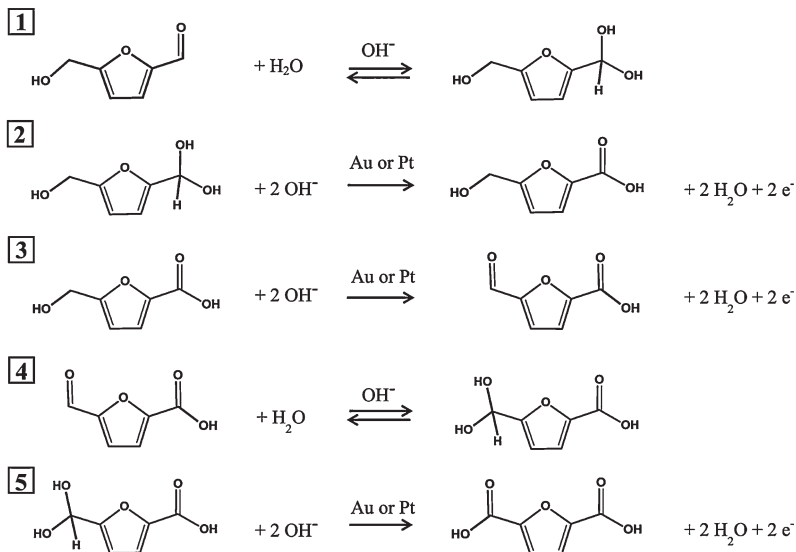
Recently, Davis et al. have compared the reaction rate and product distribution for HMF oxidation over supported metal catalysts: Pt/C, Pd/C, Au/C, Au/TiO₂ [22]. Pt and Pd were able to oxidize HFCA to FDCA, but gold catalysts demonstrated one order of magnitude higher reaction rate (1.6–5.0 s⁻¹) at the same conditions of 22 °C, 690 kPa of oxygen. The major product over the gold catalyst was HFCA. At the same conditions, increasing the base concentration (OH⁻) improved the selectivity towards FDCA formation.

The oxidation of HMF over a hydrotalcite-supported gold nanoparticle catalyst (Au/HT) in water at 95 °C under atmospheric oxygen pressure without addition of homogeneous base was recently demonstrated [23]. This study reported the oxidation as an environmentally benign process, which could be operated even at 95 °C using a conventional glass reactor with atmospheric oxygen flow. Since HT consists of layered clays with HCO₃⁻ and OH⁻ groups on the surface, it is known to exhibit high activity for base-catalyzed reactions. However, the potential for leaching of the solid base exists so the support might act as a substitute for homogeneous base in promoting catalyst activity [24].

Bimetallic Au–Cu catalysts supported on titania display higher activity compared to monometallic Au [25]. In this study the influence of base content, catalyst metal loading, temperature, and reaction time was investigated using Au–Cu/TiO₂ catalyst. It was also demonstrated that, in the absence of any catalyst, addition of base resulted in HMF degradation to form levulinic and formic acid, while in the presence of catalyst and base HMF was exclusively oxidized to HFCA and, subsequently, to FDCA. Under the optimized reaction parameters yield of FDCA was 90–99 % after 4 h at 95 °C at base loading corresponding to NaOH to HMF molar ratio of 4.

The significant role of OH-groups in the reaction mechanism was pointed out by further investigation [26]. Experiments conducted with labeled oxygen and water (¹⁸O₂, H₂¹⁶O and H₂¹⁸O) indicated that namely oxygen atoms (¹⁶O and ¹⁸O) in water were incorporated into the HMF oxidation products (HFCA and FDCA), while gaseous oxygen atoms were not found in the products. One of the explanations of the oxygen role is indirect participation in the oxidation reaction. The oxygen from the gas-phase is adsorbed on the metal surface and reduced by electrons deposited into the metal during adsorption and reaction of hydroxide ions to form peroxide species and, consequently, hydroxide ions (see Scheme 2.3).

Synthesis of FDCA is challenging due to its low solubility in most industrial solvents [27]. This difficulty can be overcome by synthesis of FDCA ester, i.e., dimethylfuroate (DMF), which is soluble in most commonly applied solvents. Casanova et al. have demonstrated excellent activity and selectivity of Au/CeO₂ catalyst in aerobic HMF oxidation to the alternative product (DMF) in base-free conditions [28].

HMF Oxidation SchemeHMF Oxidation Mechanism

Scheme 2.3 Overall reaction scheme and proposed mechanism for the oxidation of HMF in aqueous solution in the presence of excess base (OH^-) and either Pt or Au. Dioxygen (not shown) serves as a scavenger of electrons that are deposited into the metal particles during the catalytic cycle. Reproduced from Ref. [26] with permission from The Royal Society of Chemistry

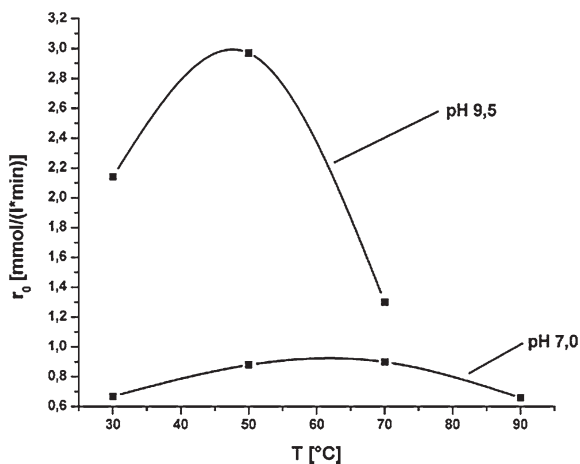
2.1.3 Selective Oxidation of Sugars

Heterogeneous catalytic oxidation of sugars over gold catalysts is very attractive, since these catalysts have demonstrated high activity and selectivity. Utilization of gold catalysts has an environmental advantage—the reaction can be performed using air or molecular oxygen as an oxidizing agent at mild reaction conditions (30–90 °C).

2.1.3.1 Selective Oxidation of Glucose

Since D-glucose is the most abundant monosaccharide in nature, its oxidation to D-gluconic acid was extensively investigated [29, 30]. The optimal conditions for D-gluconic acid formation were found to be 50 °C at pH 9.5 and 60 °C at pH 7.0 (Fig. 2.3), while reaction at higher temperatures and pH values resulted in formation of such side products as fructose, sorbitol, mannose, glycolaldehyde, and

Fig. 2.3 Initial reaction rates of D-gluconic acid formation at different reaction temperatures and pH values. Reprinted from Ref. [31], Copyright © 2004, with permission from Elsevier



maltose [31]. Kinetic studies on glucose selective oxidation resulted in different conclusions on the reaction mechanism. In [31] the reaction rate was independent of glucose concentration. However, further investigation showed the reaction rate to increase with increasing oxygen pressure from 1.5 to 9 bar and to depend on glucose concentration, having maximum at 20–30 wt. % [32]. The results fitted a Langmuir–Hinshelwood model. In another study [33] the reaction rate was found to be proportional to the oxygen pressure and increased with glucose concentration, with the energy of activation studied in the absence of mass transfer limitations estimated to be 47 kJ/mol. This value is in the same range as one reported later in [32]. According to considerations in [33], the reaction follows the Eley–Rideal mechanism, where an oxygen molecule from the fluid phase reacts directly with chemisorbed glucose.

Structure sensitivity of D-glucose oxidation to D-gluconic acid was studied in [31]. Au/C catalysts were prepared by gold sols immobilized onto a carbon support. Supported gold particles had a mean diameter of Au particles 3–6 nm with a gold loading of 0.4–0.7 wt. %. Catalytic activity of Au/C was found to have an exponential dependence on the gold specific surface area.

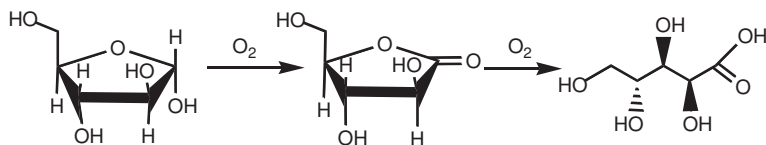
High selectivity of gold colloids in the oxidation of D-glucose to D-gluconic acid was demonstrated by Prüße and co-workers [34, 35]. Under the same conditions, Au/TiO₂ catalyst prepared by deposition–precipitation with urea (DPU) demonstrated the best performance corresponding to the complete glucose conversion with selectivity to gluconic acid of 98 %, and the specific catalytic activity of $236 \text{ mmol}_{\text{glucose}} \text{ min}^{-1} \text{ g}_{\text{metal}}^{-1}$ [34]. Development of gold on alumina catalyst preparation methods revealed a possibility to support Au particles having less than 2 nm in diameter by an incipient wetness method (IW), which has advantages over the DPU method from ecological and economical points of view. Application of 0.3 wt. % Au/Al₂O₃ catalyst prepared by IW in glucose oxidation resulted in complete selectivity to sodium gluconate with the catalyst specific activity of 1100

$\text{mmol}_{\text{glucose}} \text{ min}^{-1} \text{ g}_{\text{metal}}^{-1}$ [36]. An advanced catalyst preparation technique was shown by the group of Haruta to improve Au catalyst performance [37], where gold supported on ion-exchange resins exhibited a TOF of 7.5 s^{-1} in glucose oxidation reaction at 60°C and pH 9.5. Catalytic activity was found to increase with increasing basicity of ion-exchange resins. Relatively high catalytic activity in glucose oxidation (TOF of 11 s^{-1}) was obtained over Au/C catalysts prepared by a direct contact of gold precursor with support by grinding of carbon [38] and cellulose [39] with dimethyl Au(III) acetylacetonate. The nature of the support was found to play an important role. In [40], Au catalysts supported on TiO_2 , SiO_2 , CeO_2 were studied. Since glucose is a large multifunctional molecule, different surface arrangements and sites are needed for its adsorption. Therefore, in this series of catalysts, gold supported on silica with a mean size of gold particles ca. 10 nm was the most active catalyst [40].

Hydrogen peroxide as an oxidizing agent was investigated in [41]. In this study D-glucose oxidation by H_2O_2 was performed over 0.3 wt. % Au/ Al_2O_3 at relatively mild conditions (40°C , pH of 9). The investigation revealed that the oxidizing species were formed via H_2O_2 decomposition over the gold catalyst. Similar to aerobic oxidation reported in [32] the apparent energy of activation was 48 kJ/mol , and the reaction order for D-glucose was 0.5. In general, oxidation by hydrogen peroxide seems to be similar to aerobic oxidation, as the oxygen from gas-phase was observed to form peroxide-like species promoting oxidation.

2.1.3.2 Selective Oxidation of Arabinose, Galactose and Other Sugars

The selective oxidation of arabinose to its corresponding carboxylic acid (arabinonic acid) was studied in [42, 43]. The reaction (see Scheme 2.4) was performed at relatively moderate conditions, using oxygen as an oxidant [43]. Gold catalyst did not show any activity decline or decrease of selectivity to the desired product. It was confirmed that pH is one of the most crucial factors in the oxidation of arabinose to arabinonic acid. Generally, at low pH, the product adsorption on the catalyst strongly inhibits the reaction; therefore, the reaction is performed in the presence of base to increase the rate of the oxidation. Thus, in [43] the increase of pH value from 6 to 9 resulted in the corresponding arise of TOF from 0.015 to 0.206 s^{-1} . However, increasing of pH resulted in gold leaching from the catalyst



Scheme 2.4 Reaction scheme for the selective oxidation of arabinose to arabinogalactan and arabinonic acid by molecular oxygen. Reprinted from Ref. [43]. Copyright © 2010, with permission from Elsevier

and decrease of selectivity toward the reaction intermediate, as well as formation of by-products, which inhibit the reaction. Catalyst activity and conversion of arabinose increase as the pH increases from 6 to 9, indicating that slightly alkaline media, i.e., pH 8, is favorable. The kinetic experiments revealed as well an increase of the reaction rate with increasing of oxygen flow rate from 2.5 ml/min to 5.0 ml/min. The apparent activation energy was estimated to be ca. 24 kJ/mol in the absence of mass transfer limitations. The reaction kinetics was comprehensively studied in [44].

The influence of the catalyst support and active phase was studied in [43, 45]. The support nature and catalyst pretreatment affect the catalytic properties. Bimetallic Au–Pd catalysts demonstrated higher activity and selectivity compared to monometallic Au and Pd catalysts. The synergetic effect is attributed to the activation of arabinose by Au species, while Pd species can provide activation of oxygen.

The rate of the reaction of arabinose oxidation to arabinonic acid is apparently structure sensitive (Fig. 2.4). Dependence of catalytic activity on gold particle size has a volcano relationship with a maximum at gold cluster size ca. 2 nm. The data were also described quantitatively [46] based on a thermodynamic approach. Since the kinetic data is attributed to the average cluster size, limitations of the applied calculations are related mainly to the accuracy of the Au cluster size determination. However, the results of the calculations confirmed a good correspondence between the experimental data and the model.

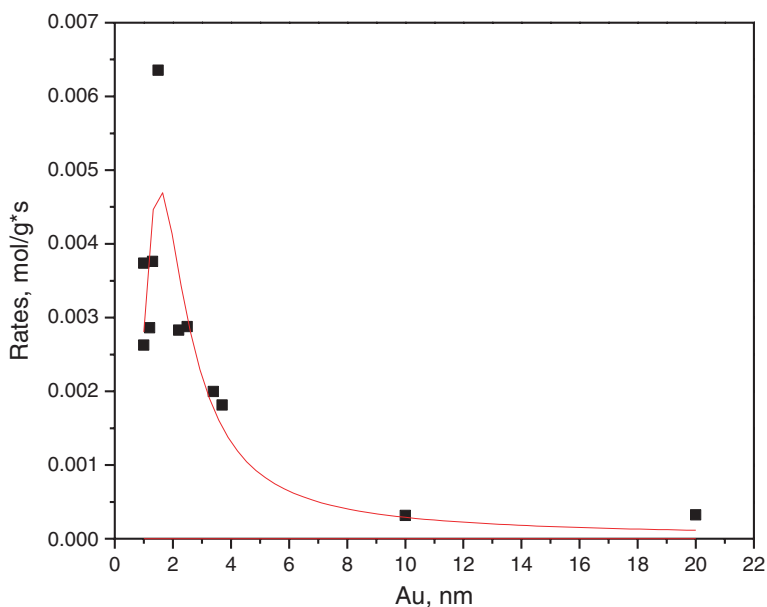
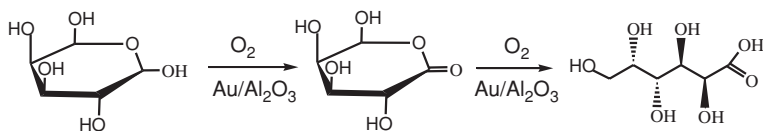


Fig. 2.4 Dependence of initial rates in arabinose oxidation on the particle size of Au/Al₂O₃ catalysts. Reprinted with permission from Ref. [46]. Copyright © 2011, American Chemical Society



Scheme 2.5 The reaction pathway of D-galactose selective oxidation over Au catalyst. Reprinted from Ref. [47], Copyright © 2011 Wiley–VCH Verlag GmbH & Co. KGaA, Weinheim

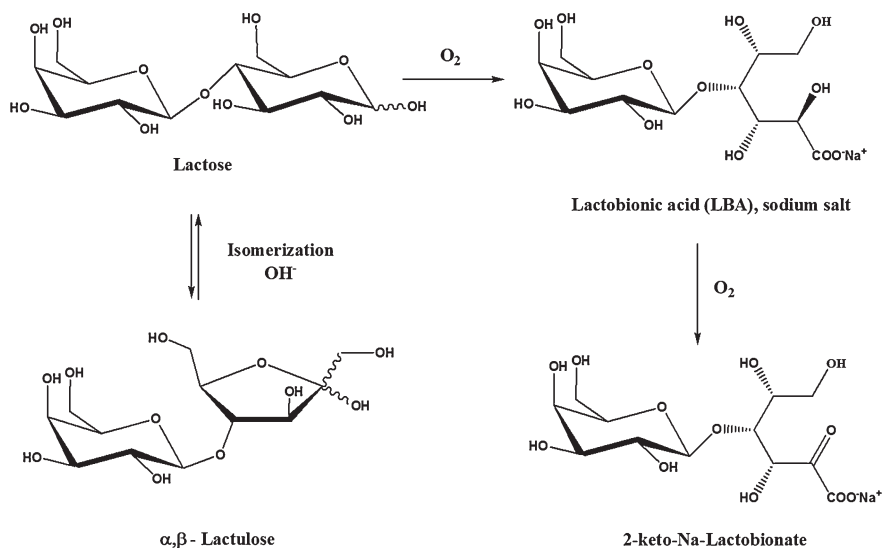
Gold catalysts exhibit high catalytic activity in the selective oxidation of D-galactose to galactonic acid (Scheme 2.5), although this reaction was not intensively investigated. In [47] the reaction was performed in a semi-batch reactor at 60 °C, under pH-s and constant oxygen flow. The reaction is structure sensitive, with Au particles of the size of 2.6 nm exhibiting the maximum activity. Similar to the case of glucose oxidation [30], alkaline conditions (pH of 8–10) accelerate the reaction rate and increase the reaction selectivity to galactonic acid, although at higher pH > 10 sugar degradation can be observed.

Other carbohydrates can be also oxidized to valuable aldonic acids over gold catalysts. The selective oxidations of various monosaccharides (ribose, xylose, lyxose, mannose, rhamnose, galactose, N-acetyl-glucosamine) and disaccharides (lactose, maltose, cellobiose, melibiose) over gold catalysts were studied in [42]. Gold catalysts demonstrated higher selectivity (ca. 100 %) to corresponding aldonic acids and higher specific catalyst activity ($6\text{--}24 \text{ mmol/min} \times g_{\text{Au}}$) compared to palladium and platinum catalysts ($1\text{--}10 \text{ mmol/min} \times g_{\text{Pt or Pd}}$) applied in the same conditions. Similar to selective oxidation of glucose and arabinose, in order to avoid molecules degradation and formation of by-products, it is preferable to conduct the reaction at low temperatures (40–60 °C) and in light alkaline media at pH 7–9.

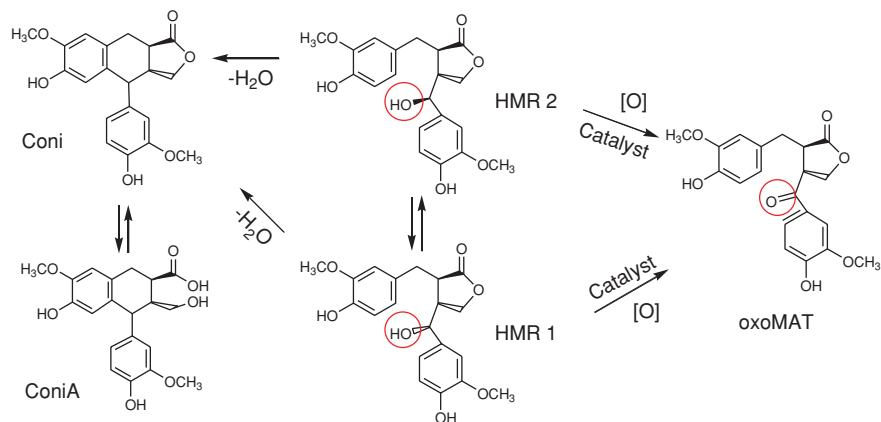
Structure sensitivity of lactose selective oxidation to lactobionic acid (Scheme 2.6) was studied. Similar to arabinose and galactose the dependence of the reaction rate on Au particle size has volcano shape with maximum at 6 nm [48]. Support does not influence the reaction selectivity. In [42] it was reported that Au/TiO₂ (gold particle size 1–2 nm) is more active in mannose oxidation, while Au/Al₂O₃ is more active in lactose oxidation.

2.2 Secondary Alcohols Oxidation

The formation of the lignan oxoMAT from the lignan HMR by light-irradiation was reported in [49], while in [50] 2,3-dichloro-5,6-dicyano-1,4-benzoquinone (DDQ) was used as an oxidizing agent. An attempt has been made to perform the reaction via heterogeneous catalysis, namely Pd/C, providing a more commercially attractive synthesis of oxoMAT. However, oxoMAT was not the only product in this reaction [51]. OxoMAT is formed via selective oxidative dehydrogenation of secondary



Scheme 2.6 The lactose oxidation over gold catalyst by molecular oxygen in the presence of base. Reprinted from Ref. [96], Copyright © 2008, with permission from Elsevier



Scheme 2.7 Reaction pathways of lignan hydroxymatairesinol (HMR) transformation over Au gold catalysts to the lignans α -conidendrin (Coni), α -conidendric acid (ConiA) and oxomatairesinol (oxoMAT). Reprinted from Ref. [53]. Copyright © 2012, with permission from Elsevier

alcohol according to the reaction network presented in Scheme 2.7. Application of heterogeneous Au catalysts was demonstrated for the first time in [52]. Gold catalysts boost the selectivity to oxoMAT up to 100 %. At the same conditions, conversion of HMR over palladium catalysts was lower than over gold ones.

Monometallic Au and bimetallic Au–Pd catalysts supported on various carriers (Al_2O_3 , TiO_2 , MgO , SiO_2 , C, La_2O_3 , CeO_2 , ZrO_2), zeolites, and mixed oxides (Al_2O_3 – CeO_2 , Al_2O_3 – CeO_2 – ZrO_2) were tested in the oxoMAT synthesis [53]. Gold catalysts exhibited a TOF to be in the range of 0.007 – 0.117 h^{-1} , while among all tested catalysts Au/ Al_2O_3 has shown the highest activity (TOF of 0.117 h^{-1}). Au/ Al_2O_3 , TiO_2 , SiO_2 , C have demonstrated 100 % selectivity towards oxoMAT. Reaction over Au/ La_2O_3 , CeO_2 , ZrO_2 catalysts led to the formation of the other lignans such as α -condendrin, α -condendric acid, and isomerization between HMR isomers. Addition of Pd did not improve the catalyst performance, the initial catalytic activity was found to be similar for mono and bimetallic catalysts. The role of the support was found to have a dominating effect on the reaction selectivity. Thus, gold supported on basic supports was less active and selective to oxoMAT, than on acidic ones. High catalytic activity was attributed to the presence of OH-groups on the support surface formed due to water adsorption on Lewis acid sites [52, 53].

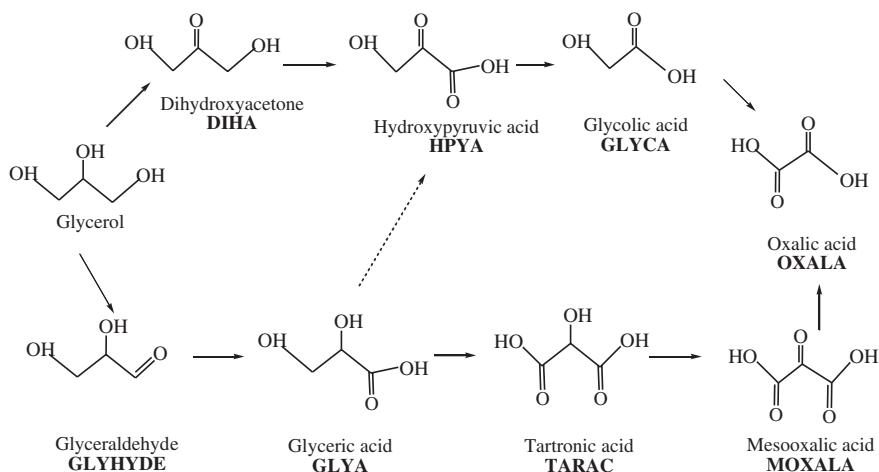
HMR extracted from wood biomass is a mixture of two diastereomers: (7R,8R,8'R)-(-)-7-allo-hydroxymatairesinol (HMR 1) and (7S,8R,8'R)-(-)-7-allo-hydroxymatairesinol (HMR 2), which exist in different conformations [54] and can be isomerized into each other. The molar ratio SRR-HMR/RRR-HMR depends on the tree species and in case of Norway spruce (*Picea abies*) knots typically is 2 mol/mol. Both isomers can be oxidized into oxoMAT over Au catalysts, while SRR-HMR is the most reactive one. The difference in the oxidation rate of each isomer was explained by possible steric hindrance and difference in the isomers energies confirmed by use of quantum chemical calculations in [55].

Synthesis of oxoMAT can be performed under aerobic and anaerobic conditions. However, the presence of oxygen significantly increases the reaction rate [52]. The reaction mechanism of aerobic and anaerobic HMR dehydrogenation was investigated [55]. Activated oxygen was found to play the essential role in the reaction, as oxygen species on the gold catalytic surface, which act as Brønsted basic sites, enhance the dehydrogenation rate [56].

A kinetic study of lignan HMR aerobic dehydrogenation was performed. The reaction order was found to be ca. 0.3–0.4 order in respect to HMR isomers and oxygen. The apparent energy of activation was estimated to be 43 kJ/mol [57]. The kinetic model of the reaction was developed. During the process the reaction rate was found to be retarded by the formed oxoMAT and impurities presented in the substrate, which was included in the model. The deactivation of the catalyst was studied in details in [58].

2.3 Polyalcohol Oxidation

Glycerol is a multifunctional molecule, and the oxidation pathway is complicated by parallel and sequential reactions (Scheme 2.8). Glyceraldehyde can be easily isomerized to dihydroxyacetone, while the oxidation of the former one is more



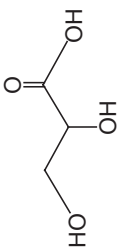
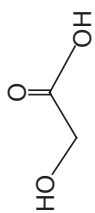
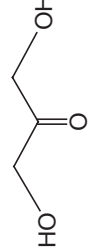
Scheme 2.8 The reaction pathway of glycerol selective oxidation. Reprinted from Ref. [84]. Copyright © 2006, with permission from Elsevier

challenged and, thus, glyceric acid is the major product in many cases. Traditional catalysts based on Pt and Pd can be deactivated due to overoxidation of their surface. However, gold catalysts were found to be more stable than Pt and Pd, and possess high selectivity. Reaction over gold catalysts can lead to products with one or two carbon atoms, as for example, glycolic acid. Subsequent oxidation of glyceric acid results in tartronic acid formation. Catalyst composition and reaction conditions were found to affect the product selectivities [59–64].

Hutchings and co-workers reported the formation of glyceric acid at selectivity of 100 % over Au/C in autoclave under 3–6 atm of oxygen, at 60 °C, while the selectivity was decreasing to 86 % at increasing of glycerol conversion from 56 to 72 % [59, 60]. In the presence of base the group of Prati observed the selectivity depends on a combination of catalyst properties, including metal type, Au particle size and support properties [61–64]. In their further study the experimental conditions were optimized [65]. The highest selectivity to glycerate was 92 % at full glycerol conversion at 30 °C under 300 kPa of oxygen and NaOH/glycerol molar ratio of 4. Furthermore, it was found, that catalysts with average Au particles size about 6 nm did not maintain the initial selectivity at full conversion, while larger particles (> 20 nm) showed constant selectivity during the reaction.

In the last years the number of papers on glycerol oxidation with oxygen is essentially increased. Gold catalyzed oxidation of glycerol using H_2O_2 as an oxidant was as well successfully performed in [66]. In this case glycolic acid was the major product (ca. 60 % yield). In Table 2.1 the reaction conditions, catalyst selection, and selectivity to different products are given based on the results published recently [67–82]. Different aspects of glycerol oxidation such as the effect of reaction conditions, catalyst, support nature, Au particle size as well as reported kinetic peculiarities discussed bellow.

Table 2.1 Selective oxidation of glycerol. Catalyst selection, reaction conditions, product selectivity at given glycerol conversion

Product	X (%)	S (%)	Reaction conditions	χ mol/mol (or pH)	Catalyst	d_{Me} (nm)	TOF (h^{-1})	References
 Glyceric acid	40	45	60 °C, 100 kPa (O_2)	pH 12	Au/C, TiO_2 , Al_2O_3 , MgO , CeO_2	2–5		[68, 85]
	10–80	50–70	35–60 °C, 1000 kPa (O_2)	2	Au/C, TiO_2 ,	2–12	100–1090	[74, 85]
	12–97	52–78	50 °C, 100–600 kPa (O_2)	0.5–4	Au–Pd/C	3.7		[79]
	50	62–83	60 °C, 500–1000 kPa (O_2)	2	Au/C	5–42	61200	[75]
	50–100	50–77	30–50 °C, 300 kPa (O_2)	4	Au–Pd/C			[71, 72]
	70–90	62	50 °C, 300 kPa (O_2)	4	Au–Pt/C	2–3	980	[73, 76]
	50	65–84	60 °C, 1000 kPa (O_2)	2	Au–Pd/C, Au/C	3–5	18000–61200	[78]
	30	40–100	60 °C, 100–300 kPa (O_2)		Au/C			[80]
 Glycolic acid	13–78	30–55	60–90 °C, 600 kPa (O_2)	2	Au/C, TiO_2 , Nb_2O_5			[82]
	70–90	40–60	60 °C, 300 kPa (O_2)	2	Au/C	5	2500–4310	[89, 92]
	100	60	H_2O_2		Au/C			[67]
	10–80	20–50	35–60 °C, 1000 kPa (O_2)	2	Au/C, TiO_2	5–12	18000–61200	[74]
 Glycolic acid	50	55–60	60 °C, 300 kPa (O_2)	0.5–2	Au/C	5–23	1080–4000	[6]
	50	36	60 °C, 100 kPa (O_2)	pH 12	Au–Pt/C			[76]
Dihydroxyacetone	93	60	60 °C, 300 kPa (O_2)	2	Au/C	5	4240	[89]

X glycerol conversion; S selectivity towards the product; d_{Me} average diameter of the supported metal; χ NaOH to glycerol molar ratio

2.3.1 Role of Base

The presence of a base is essential for glycerol oxidation. According to a commonly accepted opinion, bases promote dehydrogenation step of glycerol oxidation/dehydrogenation [6, 59, 67]. The reaction selectivity can be controlled by the amount of base. As shown in [67] the selectivity to glyceric and tartronic acid could be changed by the base amount. Glyceric acid formation was favored up to NaOH/glycerol molar ratio of 2, although with increasing of this ratio to 4, tartronic acid (product of further glyceric acid oxidation) was formed with high selectivity. At the same time the reaction rate was enhanced by increasing of base loading up to a molar ratio NaOH/glycerol of 2 and above this ratio almost did not change. Similar observation was made by the group of Prati [76].

2.3.2 Gold Particle Size Effect

The structure sensitivity of the reaction was studied by several research groups. For this purpose size of Au particles supported on carbon was varied in the range 2–45 nm [67] and 5–42 nm [82]. The results obtained in both works are similar. The smallest Au particles have demonstrated much higher activity in glycerol oxidation. However, the selectivity to glyceric acid at conversion of 30 % passed through a maximum: increased with increasing of Au particle size, reached maximum at average Au diameter 3.7 nm (75 % to glyceric acid) and followed by decreasing of selectivity to glyceric acid with increasing of Au particles size up to 42 nm. Furthermore, the smallest particles have the highest selectivity to glycolic acid—the product of C–C bond cleavage [67]. The reason for this was revealed in [74], where Ketchie et al. have observed that highly dispersed gold particles are more active in hydrogen peroxide formation during glycerol oxidation, which in turn promotes C–C cleavage. Influence of gold particle size on catalyst activity and selectivity was also evaluated using gold supported on carbon nanotubes (Au/CNT) with Au particles size 3–23 nm [82]. Dependence of turnover frequency (TOF) on gold particle size has a maximum at 5.5 nm at TOF value of $6 \pm 2.1 \times 10^{-3} \text{ h}^{-1}$. Catalyst supported on multi-walled carbon nanotubes (Au/MWCNT) has the highest total selectivity towards dihydroxyacetone and glyceric acid among tested ones (86 %).

2.3.3 Bimetallic Catalysts

Addition of Pt and Pd to Au catalysts was found to have a promoting effect in the various reactions of selective oxidation and was attributed to the synergetic effect due to alloy formation and is described in [68, 69]. The effect of bimetallic gold

catalysts on the product distribution in glycerol oxidation was also investigated. Addition of Pt and Pd was observed to improve catalyst activity and selectivity in glycerol oxidation. For example, a Au–Pd/C catalyst was shown to have higher selectivity to glyceric acid and higher activity than monometallic Au catalyst, the best results obtained under 300 kPa of oxygen, at 30–50 °C were 70–77 % selectivity to glyceric acid at 90 % conversion [70, 71]. The effect of preparation method of Au–Pt/C on the product distribution was studied in [72] at 300 kPa of oxygen, and 50 °C. The most active and selective catalyst for glyceric acid formation (62 % of selectivity) was prepared using H₂ as a reducing agent, while the other product was glycolic acid. The selectivity toward dihydroxyacetone at the expense to glyceric acid was improved from 26 % (Au/C) to 36 % (Au–Pt/C) by promoting the gold catalysts with platinum [75]. The advantage of using Au–Pd bimetallic catalysts is the catalyst stability, although some surface reconstruction and Pd leaching was observed [76]. Au–Pd catalyst has higher selectivity to glyceric acid, while it was less active [77]. Palladium was proposed to catalyze H₂O₂ decomposition formed on gold surface and hence the selectivity to glyceric acid was improved. In [74] the effect of the reaction parameters was studied using Au–Pd on activated carbon. The major products of glycerol oxidation were glyceric, glycolic and tartronic acids. It was revealed that selectivity to glyceric acid could be affected by applying different reaction conditions, thus, it increased from 52 to 80 % with: (i) decreasing of base loading (NaOH/glycerol ratio was 0.5 to 4 mol/mol); (ii) increasing substrate/metal ratio (was varied from 860 to 6900 mol/mol); (iii) increasing of oxygen pressure (from 1 to 6 bar). Catalytic activity was observed to be enhanced by loading of more catalyst and base.

2.3.4 Support Effect

The support effect on the catalyst performance was studied. The superior performance of Au/C compared to Au/TiO₂, Al₂O₃, MgO, CeO₂ in terms of activity and selectivity control was demonstrated by the group of Claus [67, 83]. Under the same experimental conditions the gold catalysts supported on carbon showed much higher activity in the liquid-phase oxidation of glycerol than magnesia and ceria supported gold catalysts [67]. Different carbon types were applied for gold catalyst preparation, and the effect of their pore structure on catalyst performance was investigated. Carbon pore structure was found to have a strong influence on Au/C catalyst activity, and in particular, supports with more micropores have demonstrated lower activity, although the product distribution was similar [75]. In [84], activity of Au/TiO₂ catalysts was thoroughly investigated. Catalysts were prepared by different methods, mainly deposition–precipitation (DP) and immobilization of gold sols. For the tested samples, gold particles were found to have two oxidation states (Au⁰, Au^{III/δ+}), while Au⁰ was considered to provide the most active sites for oxidation of glycerol. The most active catalyst was found to be Au/TiO₂ prepared by DP, followed by chemical reduction using NaBH₄, while the

selectivity to glyceric acid was obtained over less active Au/TiO₂ (DP/calced) catalyst. However, the turnover frequency (TOF) value of Au/C reported in their previous work [70] (1090 h⁻¹) was higher than TOF obtained for Au/TiO₂ catalyst prepared in similar way (178 h⁻¹) and the most active Au/TiO₂ (721 h⁻¹) (DP/NaBH₄), while the product distribution was similar in the studied cases. Thus, catalytic activity was demonstrated to be affected by the support.

Comparative catalytic studies of Au supported on Nb₂O₅, V₂O₅, Ta₂O₅, and Al₂O₃, TiO₂, C were performed [78]. Niobium oxide can reveal strong metal support interactions and is active in oxidation reactions [85]. Therefore, Au catalysts supported on group V metal oxides were tested in glycerol oxidation [78]. The reaction was conducted in the liquid-phase at NaOH/glycerol molar ratio equal to 2, at 60 and 90 °C, under 6 atm of oxygen. The main product of the reaction was glyceric acid in all studied cases. Results of this study have demonstrated that the highest conversion of glycerol was achieved over commercial Au/TiO₂, while among prepared catalysts, Au/Nb₂O₅ and Au/C demonstrated the highest glycerol conversion of 67 and 76 %, correspondingly. Moreover, the yield of glyceric acid was higher in case of niobium oxide supported gold.

Since Au/MgAl₂O₄ is a promising catalyst for gas-phase CO oxidation and liquid-phase ethanol oxidation to acetic acid [3, 4, 86], it was also investigated in liquid-phase glycerol oxidation. Selectivity was found to be correlated with the Al/Mg ratio in the support. An Al-rich surface gave the lowest C₃ product yield (glycerate and tartonate), while increasing of Mg fraction increased selectivity to C₃ products (60–70 %). Activity of the catalysts was influenced by amount of Au exposed. Therefore, catalytic behavior can be tuned by changing of spinel composition.

The relationship between carbon surface composition and Au/C catalyst performance in glycerol oxidation was studied in [87]. Carbon supports with different amounts of surface oxygenated groups were tested, while keeping their textural characteristics similar. The oxygen content on the surface had a strong influence on catalyst activity. A basic (oxygen-free) carbon support possesses a high density of π -electrons, which led to an increase in the reaction rate. However, the presence of surface functional groups did not affect the reaction selectivity. Total selectivity to glyceric acid and dihydroxyacetone was 80 %. Catalytic behavior of Au/C catalysts supported on multi-wall carbon nanotubes (CNT) and activated carbon (AC) was compared in [88]. Catalysts with similar metal loading and average Au particle size were found to have different selectivity to glyceric acid and dihydroxyacetone. A CNT-supported catalyst promoted dihydroxyacetone (60 %) formation due to preferential chemoselective orientation of glycerol for oxidation of secondary alcohol group. At the same conditions, reaction over Au/AC resulted mainly in formation of glyceric acid. More details of Au supported on multi-walled carbon nanotubes prepared by different methods evaluation were given in [82].

Gold catalysts supported on various carbonaceous materials were studied in the liquid-phase glycerol oxidation [89, 90]. Support structure affects the activity of Au particles, and then, activity and selectivity could be changed. In general, higher

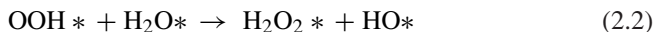
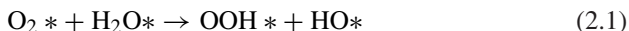
support crystallinity and smaller Au particle size, promote catalyst activity and selectivity. Similar results in terms of crystallinity were obtained in [78]. Higher activity of catalysts on supports with higher crystallinity in case of Au/C was associated with higher dispersion of Au particles.

Mesoporous carbon xerogels (CX) were considered to be promising catalyst supports for Au-catalyzed glycerol oxidation to glyceric acid, dihydroxyacetone, and glyceric acid [91]. The pore size of the support was found to have a strong influence on product selectivity. Wide pores are favorable for dihydroxyacetone formation, while narrow pores enhanced glyceric acid formation. Since pore size of CX can be easily modified, the reaction selectivity can be controlled.

Carbon-supported Au proved to be the best catalysts in glycerol oxidation due to such properties as acid and base resistance, porosity and controlled surface chemistry, and a possibility of metal recovery by combustion of the support [92, 93]. The approach to improve Au/C performance in glycerol oxidation is the synthesis of carbon materials with adjusted textural characteristics, surface chemistry and mechanical strength.

2.3.5 Kinetic Observations and the Reaction Mechanism

The effect of oxygen pressure was evaluated and glycerol oxidation rate was found to be independent of oxygen pressure in the range from 4 to 10 bar [67], 1 to 6 bar [74], 1 to 8 bar [90]. The mechanism of glycerol oxidation reaction is considered to be oxidative dehydrogenation as described in [94, 95]. Zope et al. [82] have studied liquid-phase glycerol oxidation by using labeled oxygen and water. This study indicated that during glycerol oxidation, glyceraldehyde ($\text{HOCH}_2\text{CHOHCHO}$) is the reaction intermediate produced by the initial dehydrogenation of the primary alcohol of glycerol. The base-catalyzed rapid interconversion of glyceraldehyde to dihydroxyacetone ($\text{HOCH}_2\text{COCH}_2\text{OH}$) during the oxidation reaction is involving more than two labeled oxygen atoms from water in the product. Molecular oxygen was found to play an indirect role during oxidation by forming hydrogen peroxide followed by hydroxide species formation. Oxygen activation follows formation and dissociation of hydrogen peroxide according to the reaction sequence:



Moreover, the presence of adsorbed hydroxide species could lower the energy barrier for the C–H bond activation of alkoxide intermediate to form the aldehyde. The increasing of pH results in higher glycerol conversion and decreasing of activation energy to 5–12 kJ/mol [82, 90] compared to 50 kJ/mol [67] at lower pH.

References

1. N. Yoneda, S. Kusano, M. Yasui, P. Pujado, S. Wilcher, *Appl. Catal. A* **221**, 253 (2001)
2. R. Sakamuri, Esters, organic in Kirk-Othmer Encyclopedia of chemical technology, online version on Wiley Inter Science. DOI: [10.1002/0471238961.05192005200121.a01.pub2](https://doi.org/10.1002/0471238961.05192005200121.a01.pub2)
3. C.H. Christensen, B. Jørgensen, J. Rass-Hansen, K. Egeblad, R. Madsen, S.K. Klitgaard, S.M. Hansen, M.R. Hansen, H.C. Andersen, A. Riisager, *Angew. Chem. Int. Ed.* **45**, 4648 (2006)
4. B. Jørgensen, S.E. Christiansen, M.L.D. Thomsen, C.H. Christensen, *J. Catal.* **251**, 332 (2007)
5. X. Li, E. Iglesia, *Chem. Eur. J.* **13**, 9324 (2007)
6. T. Mallat, A. Baiker, *Chem. Rev.* **104**, 3037 (2004)
7. B. Jørgensen, S.B. Kristensen, A.J. Kunov-Kruse, R. Fehrmann, C.H. Christensen, A. Riisager, *Top. Catal.* **52**, 253 (2009)
8. C. Della Pina, E. Falletta, L. Prati, M. Rossi, *Chem. Soc. Rev.* **37**, 2077 (2008)
9. A. Corma, H. Garcia, *Chem. Soc. Rev.* **37**, 2096 (2008)
10. A.S.K. Hashmi, *Chem. Rev.* **107**, 3180 (2007)
11. A.S.K. Hashmi, G.J. Hutchings, *Angew. Chem. Int. Ed.* **45**, 7896 (2006)
12. O.A. Simakova, V.I. Sobolev, K.Yu. Koltunov, B. Campo, A.-R. Leino, K. Kords, D.Yu. Murzin, *ChemCatChem* **2**, 1535 (2010)
13. V.I. Sobolev, O.A. Simakova, K.Y. Koltunov, *ChemCatChem* **3**, 1422 (2011)
14. Y. Guan, E.J.M. Hensen, *Appl. Catal. A* **361**, 49 (2009)
15. P. Verdeguer, N. Merat, A. Gaset, *J. Mol. Catal.* **85**, 327 (1993)
16. P. Vinke, H.E. van Dam, H. van Bekkum, in *New Developments in Selective Oxidation*, ed. by G. Centi, F. Trifiro (Elsevier, New York, 1990), p. 147
17. W. Partenheimer, V. Grushin, *Adv. Synth. Catal.* **343**, 102 (2001)
18. O.C. Navarro, A.C. Canos, S.I. Chornet, *Top. Catal.* **52**, 304 (2009)
19. E. Taarning, I.S. Nielsen, K. Egeblad, R. Madsen, C.H. Christensen, *ChemSusChem* **1**, 75 (2008)
20. Y.Y. Gorbanev, S.K. Klitgaard, J.M. Woodley, C.H. Christensen, A. Riisager, *ChemSusChem* **2**, 672 (2009)
21. O. Casanova, S. Iborra, A. Corma, *ChemSusChem* **2**, 1138 (2009)
22. S.E. Davis, L.R. Houk, E.C. Tamargo, A.K. Datye, R.J. Davis, *Catal. Tod.* **160**, 55 (2011)
23. N. Kumar Gupta, S. Nishimura, A. Takagaki, K. Ebitani, *Green Chem.* **13**, 824 (2011)
24. B.N. Zope, S.E. Davis, R.J. Davis *Top Catal.* **55**, 24 (2012).
25. T. Pasini, M. Piccinini, M. Blosi, R. Bonelli, S. Albonetti, N. Dimitratos, J.A. Lopez- Sanchez, M. Sankar, Q. He, C.J. Kiely, G.C. Hutchings, F. Canavi, *Green Chem.* **13**, 2091 (2011)
26. S.E. Davis, B.N. Zope, R.J. Davis, *Green Chem.* **14**, 143 (2012)
27. K. Weissermel, H.J. Arpe, *Industrial Organic Chemistry* (VCH-Wiley, Weinheim, 1997), p. 225
28. O. Casanova, S. Iborra, A. Corma, *J. Catal.* **265**, 109 (2009)
29. A. Corma, S. Iborra, A. Velty, *Chem. Rev.* **107**, 2411 (2007)
30. C. Baatz, U. Prüe, *Catal. Today* **122**, 325 (2007)
31. Y. Önal, S. Schimpf, P. Claus, *J. Catal.* **223**, 122 (2004)
32. U. Prüe, M. Herrmann, C. Baatz, N. Decker, *Appl. Catal. A* **406**, 89 (2011).
33. P. Beltrame, M. Comotti, C. Della Pina, M. Rossi, *Appl. Catal. A* **297**, 1 (2006)
34. A. Mirescu, H. Berndt, A. Martin, U. Prüe, *Appl. Catal. A* **317**, 204 (2007)
35. C. Baatz, N. Thielecke, U. Prüe, *Appl. Catal. B* **70**, 653.
36. C. Baatz, U. Prüe, *J. Catal.* **249**, 34 (2007)
37. T. Ishida, S. Okamoto, R. Makiyama, M. Haruta, *Appl. Catal. A* **353**, 243 (2009)
38. H. Okatsu, N. Kinoshita, T. Akita, T. Ishida, M. Haruta, *Appl. Catal. A* **369**, 8 (2009)
39. T. Ishida, H. Watanabe, T. Bebeko, T. Akita, M. Haruta, *Appl. Catal. A* **377**, 42 (2010)
40. T. Benkó, A. Beck, O. Geszti, R. Katona, A. Tungler, K. Frey, L. Gucci, Z. Schay, *Appl. Catal. A* **388**, 31 (2010)
41. R. Saliger, N. Decker, U. Prüe, *Appl. Catal. B* **102**, 584 (2011).
42. A. Mirescu, U. Prüe, *Appl. Catal. B* **70** (2007) 644

43. B. Kusema, B.C. Campo, P. Maki-Arvela, T. Salmi, D.Yu. Murzin, *Appl. Catal. A* **386**, 101 (2010)
44. B. Kusema, J.-P. Mikkola, D.Yu. Murzin, *Catal Sci & Technol* **2**, 423 (2012)
45. E. Smolentseva, B.T. Kusema, S. Beloshapkin, M. Estrada, E. Vargas, D.Yu. Murzin, F. Castillon, S. Fuentes, A. Simakov, *Appl. Catal. A* **392**, 69–79 (2011)
46. O.A. Simakova, B.T. Kusema, B.C. Campo, A.-R. Leino, K. Kordas, V. Pitchon, P. Mäki-Arvela, D.Yu. Murzin, *J. Phys. Chem. C* **115**, 1036 (2011)
47. B.T. Kusema, B.C. Campo, O.A. Simakova, A.-R. Leino, K. Kordas, P. Mäki-Arvela, D.Yu. Murzin, *ChemCatChem* **3**, 1789 (2011)
48. L.-F. Gutierrez, S. Hamoudi, K. Belkacemi, *Appl. Catal. A* **402**, 94 (2011)
49. F. Kawamura, M. Miyachi, S. Kaway, *J. Wood Sci.* **44**, 47 (1998)
50. P. Eklund, A. Lindholm, J.-P. Mikkola, A. Smeds, R. Lehtilä, R. Sjöholm, *Org. Lett.* **5**, 491 (2003)
51. H. Markus, A.J. Plomp, T. Sandberg, V. Nieminen, J.H. Bitter, D.Yu. Murzin, *J. Mol. Catal. A* **274**, 42 (2007)
52. O.A. Simakova, E.V. Murzina, P. Mäki-Arvela, A.-R. Leino, B.C. Campo, K. Kordas, S. Willför, T. Salmi, D.Yu. Murzin, *J. Catal.* **282**, 54 (2011)
53. O.A. Simakova, E. Smolentseva, M. Estrada, E.V. Murzina, S. Willför, A.V. Simakov, D.Yu. Murzin, *J. Catal.* **291**, 95 (2012)
54. G. Li Manni, G. Barone, D. Duca, D.Yu. Murzin, *J. Phys. Org. Chem.* **23**, 141 (2010)
55. A. Prestianni, F. Ferrante, O. Simakova, D. Duca, D.Yu. Murzin, *J (Mol, Catal, 2012)*. (submitted)
56. Z. Martinez-Ramirez, S.A. Jimenez-Lam, L.C. Fierro-Gonzalez, *J. Mol. Catal. A* **344**, 47 (2011)
57. O.A. Simakova, E.V. Murzina, J. Wärnå, D.Yu. Murzin (2012) (submitted).
58. O.A. Simakova, E.V. Murzina, A.-R. Leino, P. Mäki-Arvela, D.Yu. Murzin, *Catal. Lett.* **142**, 1011 (2012)
59. S. Carrettin, P. McMorn, P. Johnston, K. Griffin, G.J. Hutchings, *Chem. Commun.* **696**, 24 (2002).
60. S. Carrettin, P. McMorn, P. Johnston, K. Griffin, C.J. Kiely, G.J. Hutchings, *Phys. Chem. Chem. Phys.* **5**, 1329 (2003)
61. L. Prati, M. Rossi, *J. Catal.* **176**, 552 (1998)
62. C. Bianchi, F. Porta, L. Prati, M. Rossi, *Top. Catal.* **13**, 231 (2000)
63. S. Biella, L. Prati, M. Rossi, *Inorg. Chem. Acta* **349**, 253 (2003)
64. C. Bianchi, S. Biella, A. Gervasini, L. Prati, M. Rossi, *Catal. Lett.* **85**, 91 (2003)
65. F. Porta, L. Prati, *J. Catal.* **224**, 397 (2004)
66. M. Sankar, N. Dimitratos, D.W. Knight, A.F. Careley, R. Tiruvalam, C.J. Kiely, D. Thomas, G.J. Hutchings, *ChemSusChem* **2**(12), 1145 (2009)
67. S. Demirel-Gülen, M. Lucas, P. Claus, *Catal. Today* **102–103**, 166 (2005)
68. L. Guzzi, *Catal. Today* **53**, (2005) 53 and cited therein references.
69. M. Chen, D. Kumar, C.W. Yi, D.W. Goodman, *Science* **310**, 291 (2005)
70. C.L. Bianchi, P. Canton, N. Dimitratos, F. Porta, L. Prati, *Catal. Today* **102–103**, 203 (2005)
71. D. Wang, A. Villa, F. Porta, D. Su, L. Prati, *Chem. Commun.* (2006) 1956.
72. N. Dimitratos, C. Messi, F. Porta, L. Prati, A. Villa, *J. Mol. Catal. A* **256**, 21 (2006)
73. W.C. Ketchie, M. Murayama, R.J. Davis, *Top. Catal.* **44**, 307 (2007)
74. W.C. Ketchie, Y.-L. Fang, M.S. Wong, M. Murayama, R.J. Davis, *J. Catal.* **250**, 94 (2007)
75. S. Demirel, K. Lehnert, M. Lucas, P. Claus, *Appl. Catal. B* **70**, 637 (2007)
76. L. Prati, A. Villa, F. Porta, Di Mang, D. Su, *Catal. Today* **122**, 386 (2007)
77. W.C. Ketchie, M. Murayama, R.J. Davis, *J. Catal.* **250**, 264 (2007)
78. N. Dimitratos, A. Villa, L. Prati, *Catal. Lett.* **133**, 334 (2009)
79. S.D. Pollington, D.I. Enache, P. Landon, S. Meenakshisundaram, N. Dimitratos, A. Wagland, G.J. Hutchings, E.H. Stitt, *Catal. Today* **145**, 169 (2009)
80. B.N. Zope, D.D. Hibbitts, M. Neurock, R.J. Davis, *Science* **330**, 74 (2010)
81. I. Sobczak, K. Jagodzinska, M. Ziolek, *Catal. Today* **158**, 121 (2010)
82. E.G. Rodrigues, S.A.C. Carabineiro, J.J. Delgado, X. Chen, M.F.R. Pereira, J.J.M. Órfão, *J. Catal.* **285**, 83 (2012)

83. S. Demirel, P. Kern, M. Lucas, P. Claus, *Catal. Today* **122**, 292 (2007)
84. N. Dimitratos, A. Villa, C.L. Bianchi, L. Prati, M. Makkee, *Appl. Catal. A* **311**, 185 (2006)
85. I. Nowak, M. Ziolek, *Chem. Rev.* **99**, 3603 (1999)
86. W.C. Li, M. Comotti, A.H. Lu, F. Schüth, *Chem. Commun.* **1772** (2006) .
87. E.G. Rodrigues, M.F.R. Pereira, J.J. Delgado, X. Chen, J.J.M. Órfão, *J. Catal.* **281**, 119 (2011)
88. E.G. Rodrigues, M.F.R. Pereira, J.J. Delgado, X. Chen, J.J.M. Órfão, *Catal. Commun.* **16**, 64 (2011)
89. S. Gil, L. Muñoz, L. Sanchez-Silva, A. Romero, J.L. Valverde, *Chem. Eng. J.* **172**, 418 (2011)
90. S. Gil, M. Marchena, L. Sanches-Silva, A. Romero, P. Sánchez, J.L. Valverde, *Chem. Eng. J.* **178**, 423 (2011)
91. E.G. Rodrigues, M.F.R. Pereira, J.J.M. Órfão, *Appl. Catal. B* **115–116**, 1 (2012)
92. G. Rodríguez-Reinoso, *Carbon* **36**, 159 (1998)
93. P. Serp, M. Corrias, P. Kalck, *Appl. Catal. A* **253**, 337 (2003)
94. J.W. Nicoletti, G. Whitesides, *J. Phys. Chem.* **93**, 759 (1989)
95. M. Besson, P. Gallezot, *Catal. Today* **57**, 127 (2000)
96. A.V. Tokarev, E.V. Murzina, J.-P. Mikkola, J. Kuusisto, L.M. Kustov, D.Yu. Murzin, *Chem. Eng. J.* **134**, 153 (2007)

Biomass Processing over Gold Catalysts

Simakova, O.A.; Davis, R.J.; Murzin, D.Y.

2013, VIII, 54 p. 24 illus., 7 illus. in color., Softcover

ISBN: 978-3-319-00905-6